Analysis of solid-state transformer interfaced with renewable energy systems in Microgrid

R.SATHISHKUMAR[1], V.CHANDRASEKARAN[2], V.MALATHI[3]
[1] *Faculty, Department of Electrical and Electronics Engineering,*
Anna University, Regional Campus Madurai, INDIA
[2] *Assistant Professor, Department of Electrical and Electronics* Engineering,
Velammal College of Engineering and Technology, Madurai, Tamilnadu.
[3] *Professor,Department of Electrical and Electronics Engineering*,
Anna University, Regional Campus Madurai, INDIA

[1]*rskgct@gmail.com,* [2]*Chander2sow@gmail.com,*[3]*vmeee@autmdu.ac.in*

***Abstract*— The reduction of multiple reverse conversions in an individual AC or DC microgrid will be analysed through Solid State Transformer (SST). It also facilitates connections from wind and solar power generation to microgrid. The SST interfaced with renewable energy system in microgrid system and its centralized power management strategy is proposed. The proposed AC microgrid system can access the distribution system without bulky transformers and can manage both the central grid and renewable systems. Wind and solar power are uncontrollable resource and also makes a challenging integration for the micro grid, particularly in terms of stability and power quality. The SST interfaced Renewable energy systems such as wind and solar power are proposed with the integrated functions of active power transfer, reactive power compensation, and voltage conversion. The SST acts as an energy router and assure for the benefit of the future residential systems. This system is modeled and simulated using Matlab /Simulink software such that, it can be suitable for modeling some kind of wind and solar power configurations. To analyze more deeply about the performance of the wind and solar system, both the normal and fault conditions will be applied.**

Keywords-AC Microgrid-three phase solid state transformer (SST)-Wind generation –solar generation-Grid connection

I. INTRODUCTION

In recent years, the complexity of the electrical grid has grown due to the increased use of renewable energy and other distributed generation sources. Distributed generation (DG) is getting more and more attention along with the rapid development for renewable energy technology in the last decade. Since the output power of distributed renewable energy resource (DRER) power depends on some unpredictable conditions of nature, such as solar irradiation and wind speed, supplying a reliable and qualified power based on DG is the major challenge for engineers, and microgrid provide a promising solution. Power electronic-based DRERs and distributed energy storage devices (DESDs) constitute the microgrid, which can not only deliver flexible and reliable power to the conventional grid, but can also operate in islanding mode in rural areas [1]. To adjust with this complexity, new technologies are required for better control and a more reliable operation of the grid. One of such technologies is the solid-state transformer (SST). The SST technology is quite new and therefore the knowledge on the behaviour of these systems in the grid is rather limited [2],[3].

The SST not only decreases in volume and weight compared with conventional transformer ,but it can also behave like smart transformer with the advantage of power flow control ,reactive power compensation capability and potential fault current limitation. Besides, the regulated the low voltage DC/AC bus of SST could be used as an interface to renewable resources and storage devices, such as wind, solar, charging stations and Dc microgrid[3]. The motivation and contribution of this paper is to analysis the performance of SST interfaced PMSG wind generator and solar with central grid into AC microgrid system. The entire system responds under normal and fault condition different operating such as wind, solar and central grid sources are modeled and simulated using MATLAB/Simulink software.

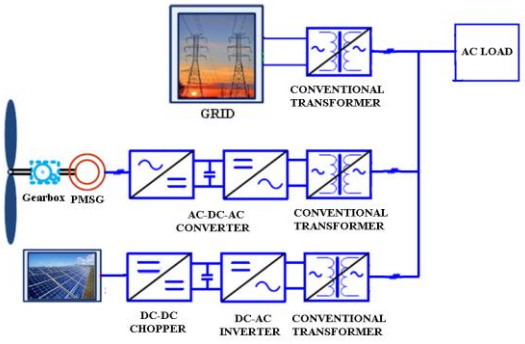

Fig.1. Conventional AC based microgrid system

Fig.1 The conventional PMSG wind and photovoltaic (PV) system integration of AC microgrid configuration, which consists of a full power rated back-to-back converter, and a step-up line frequency AC transformer. The bulky low frequency transformer increases /decreases the voltage to the required distribution voltage level. This configuration has been widely adopted in the most prevalent wind farms in a real industry application. Recently, research has been carried out to eliminate the bulky low frequency AC transformer in wind generation system [4]. Proposes a transformer-less wind generator system and PV system. Also, targeting the wind farm and solar [5], presents a new cascaded current source converter configuration, where the bulky converter substation is not needed. The SST interfaced PMSG wind and solar energy conversion system is proposed and designed in this research as a specifically different and novel alternative.

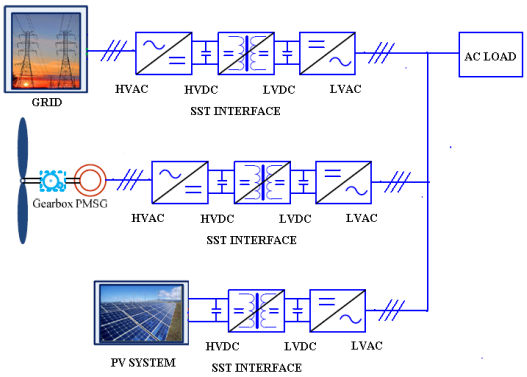

Fig.2. Proposed solid state transformer interfaced with renewable energy systems in microgrid

Fig.2. The high frequency DC/DC transformer, which effectively reduces the traditional transformer size. In this configuration, three-phase PWM rectifier is used to harness the converted wind energy. The dual active bridge (DAB) stage functions for voltage step-up/Step down, high voltage isolation and DC bus maintenance [6]. In spite of electrical isolation and voltage level conversion, advantages such as small size, light weight, power factor adjustment, power flow control, and fault diagnosis are also gained thanks to the powerful control features of SST [7-13]. This paper analysis the integration of the SST interfaced with the PMSG system and PV system to distribution in microgrid. In central grid source, bi-directional power flow to microgrid using SST is simulated.

II. SYSTEM MODELING

A. Modeling of Solid State Transformer

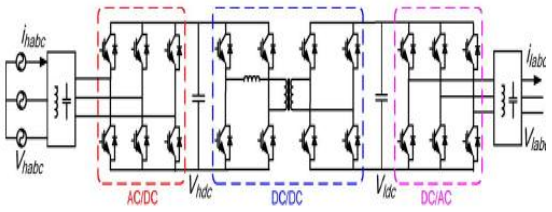

Fig.3 three phase solid state transformer

The studied system topology configuration is shown in Fig. 3. This consists of rectifier, DAB, and inverter stage. The single phase SST has been modeled in the mathematical equation. In practice, this could easily be expanded to the three phase version. The differential equations describing the inverter average model are:

$$\frac{di_{lac}}{dt} = \frac{v_{ldc}}{L_l} D - \frac{v_{lac}}{L_l} - \frac{R_h}{L_h} i_{lac} \tag{1}$$

$$\frac{dV_{ldc}}{dt} = \frac{v_{ldc}}{R_L C_l} - \frac{Di_{lac}}{C_l} \tag{2}$$

where, i_{lac} is the single-phase distribution line input current, v_{lac} is single-phase distribution line input voltage, v_{ldc} is the rectifier DC bus voltage, R_{lis} the input line resistance, L_l is the input inductor, C_l is the rectifier DC capacitor, R_L is the rectifier equivalent output load resistance, and D is the PWM duty cycle. As the single phase dq vector control method will be applied to the rectifier, an imaginary phase which is 90 degree lagging phase A needs to be hypothesized. Then combining the imaginary phase differential equation, the expressions in the dq rotational reference frame are obtained after reference transformation as (3) and (4). Interested readers are referred to [9] for the detailed derivations.

$$\frac{d}{dt}\begin{bmatrix} i_{ld} \\ i_{lq} \end{bmatrix} = \frac{V_{ldc}}{L_l}\begin{bmatrix} d_{ld} \\ d_{hq} \end{bmatrix} - \frac{1}{L_l}\begin{bmatrix} v_{ld} \\ v_{lq} \end{bmatrix} - \begin{bmatrix} \frac{R_l}{L_l} & -\omega \\ \omega & \frac{R_l}{L_l} \end{bmatrix} \tag{3}$$

$$\frac{dV_{ldc}}{dt} = \frac{V_{ldc}}{R_L C_l} - \frac{1}{2C_l}\begin{bmatrix} d_{ld} \\ d_{lq} \end{bmatrix}^T \begin{bmatrix} i_{ld} \\ i_{hq} \end{bmatrix} \tag{4}$$

The angular frequency $\omega=2\pi f$, where f is line frequency of input AC voltage. The rectifier regulates the high voltage DC link and controls the input reactive power, while the low DC bus is maintained by the DAB converter. From Fig. 3, we could see that the DAB consists of a high voltage H-bridge, a high frequency transformer, and a low voltage H-bridge. Zero voltage switching is applied for all the DAB switches, which could reduce the active switch voltage stress and thus lessen the switching loss. The amount of power transferred by DAB is given by

$$P = \frac{v_{hdc} v_{ldc}}{2Lf_s} - d_{DAB}(1 - d_{DAB}) \tag{5}$$

where, v_{ldc} is the low voltage DC bus voltage, L is the transformer leakage inductance, fs is DAB switching frequency, and d_{DAB} is the ratio of time delay of the two bridges to half switching period.

B. Modeling wind Turbine and Drive train

The mechanical power that a wind turbine extracts from wind could be considered as follows:

$$P_m = \frac{\pi}{2} \rho R^2 V_W^3 C_p(\lambda, \beta) \quad (6)$$

where, ρ is air density (Kg/m3); R is turbine blade radius (m), VW is wind speed (m/s), C_P is power coefficient of wind turbine, which is a function of both tip-speed ratio (TSR) λ and the turbine blade pitch angle β.

λi is defined as

$$\frac{1}{\lambda_i} = \frac{1}{\lambda_i + .08\beta} - \frac{0.035}{\beta^3 + 1} \quad (7)$$

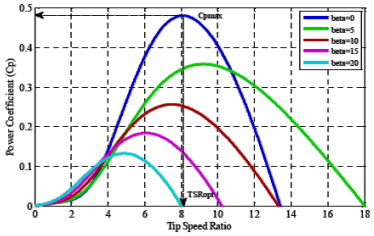

Fig..4. C_p-λ curve with different pitch angle

where $\lambda = R\omega / VW$. ω is turbine rotor rotational speed (rad/s). Fig. 4 describes the CP-λ characteristics for the studied wind turbine, under the same wind speed. It is seen that, as β increases, CP decreases. With each β, there is an optimal λ value which corresponds to the optimal operation point. In Fig. 4, the wind turbine generator system modeling also takes the gearbox into consideration. The presence of gearbox makes the shaft relatively soft, and hence, a two-mass drive train model has been adopted to better describe the drive train model. The first mass is made of the lumped inertia of the turbine, part of gearbox and the low-speed shaft, while the second one consists of the generator mass, high-speed shaft and the other part of gearbox.

The dynamic equations are obtained from Newton's equations of motion for each mass [12]:

$$2H_t \frac{d\omega_t}{dt} = T_m - T_{sh} \quad (8)$$

$$2H_g \frac{d\omega_r}{dt} = T_{sh} - T_e \quad (9)$$

$$\frac{1}{\omega_{eB}} \frac{d\theta_{tw}}{dt} = \omega_t - \omega_r \quad (10)$$

where Ht is the inertia constant of the turbine, Hg is the inertia constant of the PMSG, ω_t is the angular speed of the wind turbine in p.u., ωr is the rotor speed of the PMSG in p.u., ω_{eB} is the electrical base speed, θtw is the shaft twist angle, and T_m, Te are wind turbine and generator torque respectively.

C. Modeling of PMSG

With the aim of the generator control system design, the dynamic state voltage equations of the generator, are expressed in the rotor-oriented dq-reference frame by means of the generator principle [12];

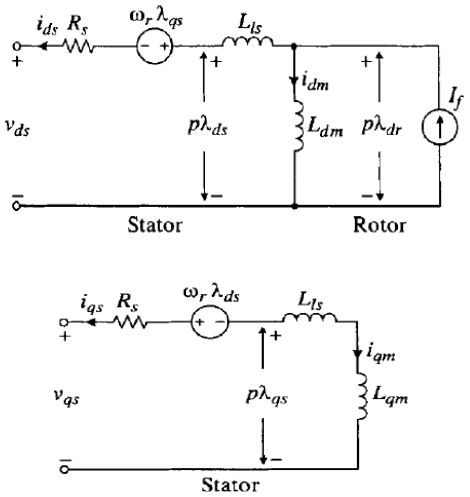

Fig.5. Equivalent circuit in dq model of PMSG

$$V_{sd} = -R_s i_{sd} - \frac{d}{dt}\lambda_{sd} - \omega_r \lambda_{sq} \quad (11)$$

$$V_{sq} = -R_s i_{sq} - \frac{d}{dt}\lambda_{sq} + \omega_e \lambda_{sd} \quad (12)$$

The stator flux components are:

$$\lambda_{sd} = L_{sd} i_{sd} + \lambda_f \quad (13)$$

$$\lambda_{sq} = L_{sq} i_{sq} \quad (14)$$

where R_s is the stator resistance, and v_{sd}, v_{sq}, i_{sd}, i_{sq}, λ_{sd}, λ_{sq}, L_{sd} and L_{sq} are the d and q axis components of instantaneous stator voltage, current, flux and inductance; λ_f is the flux linkage produced by the permanent magnet. Taking the studied surface-mounted permanent magnet machine into consideration, the electromagnetic torque T_e, stator active

$$T_e = \frac{3}{2} p \lambda_f i_{sq} \quad (15)$$

$$P_s = T_e \omega_r = \frac{3}{2}(v_{sd} i_{sd} + v_{sq} i_{sq}) \quad (16)$$

$$Q_s = \frac{3}{2}(v_{sd} i_{sq} - v_{sq} i_{sd}) \quad (17)$$

D. Modeling of Photovoltiac (PV) system

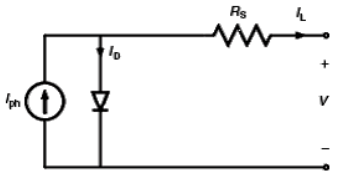

Fig.6. Model for a PV cell

The relationship between current and voltage may be determined from the diode characteristic equation

$$I = I_{ph} - I_o \left[exp\left(\frac{qV}{nkT}\right) - 1 \right] = I_{ph} - I_d \qquad (18)$$

where I_0 is the reverse saturation current, q is the charge carrier, k is the Boltzman constant, T is the cell temperature, and n is the ideality factor. The PV module has two limiting components fig.6. open-circuit voltage (*V*oc) and short-circuit current (*I*sc).

To determine *I*sc, set $V = 0$ and *I*sc = *I*ph Eq. (18), and this value changes proportionally to the cell irradiance. To determine *V*oc, set the cell current $I_L = 0$, hence Eq. (19) leads to

$$V_{oc} = \frac{nkT}{q} ln\left[\frac{I}{I_0}\right] \qquad (19)$$

The PV module can also be characterized by the maximum point when the product (V_{mp} (voltage, where power is maximum) × I_{mp} (current, where power is maximum) is at its maximum value. The maximum power output is derived by

$$\frac{d(V \times I)}{dt} = 0 \qquad (20)$$

and

$$V_{mp} = V_{oc} - \frac{kT}{q} ln\left[\frac{V_{mp}}{nkT/q} + 1\right] \qquad (21)$$

A PV module is normally rated using its*W*p, which is normally 1 kW/m2 under standard test conditions (STC), which defines the PV performance at an incident sunlight of 1000W/m2, a cell temperature of 25◦C (77◦F), and an air mass (AM) of 1.5. The product (*V*mp×*I*mp) is related to the product generated by ($V_{OC} \times I_{SC}$) by a fill factor (FF) that is a measure of the junction quality and series resistance, and it is given by

$$FF = \frac{V_{mp} \times I_{mp}}{V_{oc} \times I_{sc}} = 0 \qquad (22)$$

To achieve the desired voltage and current levels, solar cells are connected in series (*N*s) and parallel (*N*p) combinations forming a PV module.

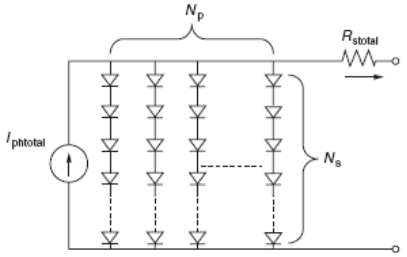

Fig..7. PV module circuit model

This model is shown in Fig.7. In order to obtain the appropriate voltages and outputs for different applications, single solar cells are interconnected in series (for larger voltage) and in parallel (for larger current) to form the photovoltaic module.

PV modules share a common DC bus through power electronic interface, in DAB topology.DAB achieves zero voltage switching (ZVS) in a wide operation range, guaranteeing the high efficiency. PV panel current and voltage are sensed for control purpose. Incremental and Conductance method is implemented in order to find the optimum operating voltage and achieve MPPT [5].

III. SYSTEM CONTROL PRINCIPLE

The block diagram of the proposed solid state transformer interfaced wind energy conversion system, PV system and central grid in microgrid is given in fig. 2. This system design principle obviously achieves a compact size and high power density renewable integration by directly interfacing the solid state electronics converted energy to the distribution line. Moreover, this configuration features the grid connected reactive power regulation and fault tolerant operation function, which are now-a-days becoming critical for renewable energy applications. The system also enables integration with a AC grid with electrical isolation.

A. Wind Energy Controls System

Due to the nature of wind, the rotor speed should be adjusted to follow wind speed change to capture the maximum power possible. In practice, the measurement of the wind speed is unreliable. It can be seen that the mechanical power converted from wind is proportional to the cube of the rotor speed. The correct combination of rotor speed and the pitch angle under different wind speeds will produce the desired amount of power.

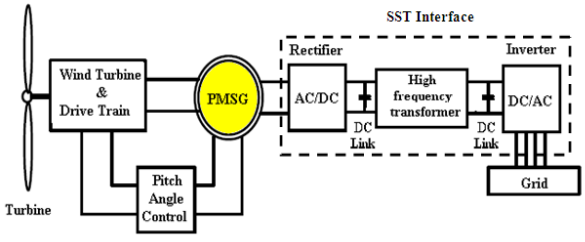

Fig.8. SST interface with wind energy conversion control system.

The PMSG speed controller ensures that the desired generator speed is maintained. The rectified DC bus voltage V_{ldc} is regulated by the DAB stage with phase shift control strategy under different load conditions as well as wind power injection. The PCC side DC bus voltage v_{hdc} is regulated by the active current i_{hd}, while the reactive current i_{hq} is controlled to a certain value for reactive power compensation and zero for unity power factor operation. The control logic demonstrates the dual loop design in the *dq* coordinate reference.

The permanent magnet synchronous generator (PMSG) has several significant advantageous properties. The construction is simple and does not required external magnetization, which is important especially in stand-alone wind power applications and also in remote areas where the grid cannot easily supply the reactive power required to magnetize the induction generator. Similar to the previous externally supplied field current synchronous generator, the most common type of power conversion uses a bridge rectifier (controlled/uncontrolled), a DC link, and inverter as shown in fig. 8. The wind energy system where a PMSG is connected to a three-phase SST. As a result, this configuration have been considered for small size wind energy conversion systems (smaller than 50kW).

B. PV Energy Controls System

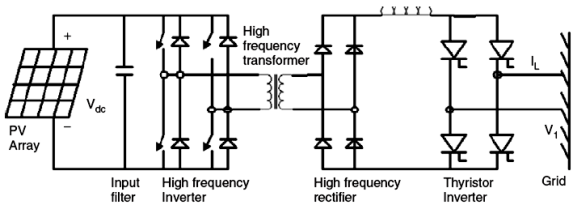

Fig.9. PV inverter with high frequency transformer

The 50 Hz transformer for a standard PV inverter with PWM switching scheme can be very heavy and costly. While using frequencies more than 20 kHz, a ferrite core transformer can be a better option . A circuit diagram of a grid-connected PV system using high frequency transformer is shown in the fig.9. The capacitor on the input side of high frequency inverter acts as the filter. The high frequency inverter with PWM is used to produce a high frequency AC across the primary winding of the high frequency transformer. The secondary voltage of this transformer is rectified using high frequency rectifier. The DC voltage is interfaced with a thruster inverter through low-pass inductor filter and hence connected to the grid. The line current is required to be sinusoidal and in phase with the line voltage.

This control system generates the waveforms and regulates the waveform amplitude and phase to control the power flow between the inverter and the grid. The grid-interfaced PV inverters, voltage-controlled VSI (VCVSI), or current-controlled VSI (CCVSI) have the potential of bi-directional power flow. They cannot only feed the local load but also can export the excess active and reactive power to the utility grid.

The control diagram indicates the basic operation of the power conditioning system. The two outer control loops operate to independently control the real and reactive power flow from the PV inverter. The real power is controlled by an outer MPPT algorithm with an inner DC link voltage control loop providing the real current magnitude request *Ip* and hence the real power export through PV converter is controlled through the DC link voltage regulation. The DC link voltage is maintained at a reference value by a PI control loop, which gives the real current reference magnitude as its output.

Synchronization of inverter with the grid is performed automatically and typically uses zero crossing detection on the voltage waveform. An inverter has no rotating mass and hence has no inertia. Synchronization does not involve the acceleration of a rotating machine. Consequently, the reference waveforms in the inverter can be jumped to any point required within a sampling period. If phase-locked loops are used, it could take up a few seconds. Phase-locked loops are used to increase the immunity to noise. This allows the synchronization to be based on several cycles of zero crossing information.

C. Cenrtral Controller System.

The SST interfaced with wind, solar and central grid source in AC microgrid. The GRID- SST(bi-directional inverter) can inject power to central grid when excess energy is available from the renewable sources. In another way, The GRID- SST can absorb power from the central grid, when renewable source is not available in microgrid. The SST may also provide “peak shaving” as part of a control strategy when the renewable source is overloaded. The renewable energy sources (RES) such as photovoltaic and wind are coupled on the AC microgrid through SST. Grid integration of RES results in to manage the critical load for purpose of RES repair and maintenance. This is one type of configuration in controllers model for Parallel hybrid energy systems shown in fig. 10.

The central grid power rather than their individual component ratings limit the maximum load that can be supplied. The capability to synchronize the SST with central grid allows greater flexibility to optimize the operation of the system. By using the same power electronic devices for both inverter and rectifier operation, the number of system components is minimized

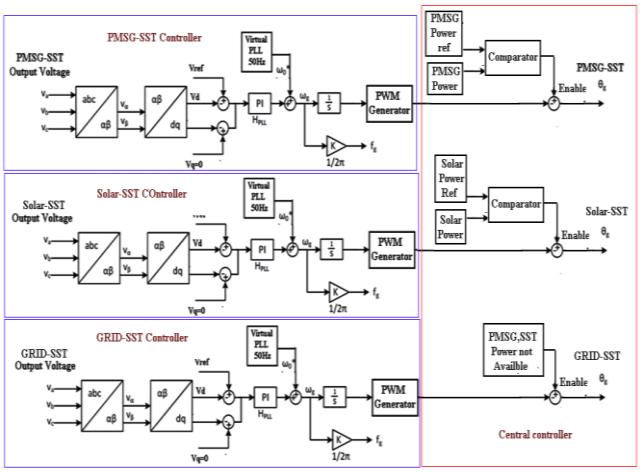

Fig.10. Model of Controllers.

This highly integrated system concept has advantages over a more modular approach to system design, but it may prevent convenient system upgrades when the load demand increases. The parallel configuration offers a number of potential advantages over other system configurations.

IV. SIMULATION VERIFICATION

A Three phase 10KVA/530V PMSG-SST,10.5 KW/435V PV-SST and 10kVA/11KV central grid source interfaced with SST are designed to constitute the 3 phase AC microgrid with load and 11KV grid connected load. The AC microgrid connected with 3 phase AC load the (2.5+2.0+2.0) 6.5 KW/(.25+.2+.2)0.70 KVAR load , 415V, 50Hz and Grid connected AC load of 2KW/0.20KVAR, 11KV,50Hz shown in fig.11. Three-phase SST was designed for Dual active bridge (DAB) converters are connected with dc link. In the last stage, three-phase inverter is connected to provide 415-V AC Microgrid. The PV generation unit is operating with MPPT control, the maximum power is 10.5KW and the corresponding MPPT voltage is about 415V. When the PV source(DC) is converted into 3phase AC supply through SST.

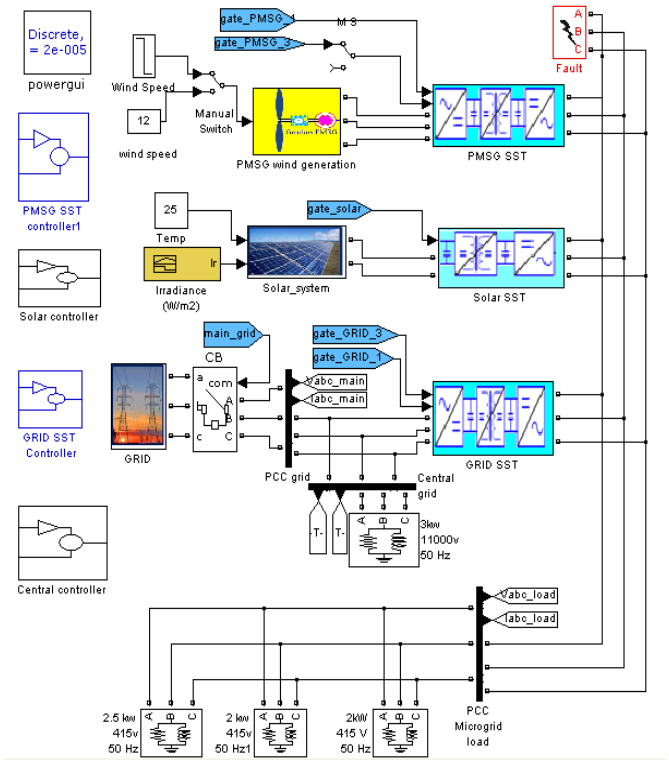

Fig.11. Simulation Model of solid state transformer interfaced wind energy conversion system , PV system and central grid in microgrid.

In AC microgrid, it operates in different mode operation such as like Wind generation mode, PV generation mode and grid connection mode.

A. Wind generation mode

10KVA PMSG supplies power to the microgrid through PMSG-SST.PMSG-SST is maintaining the 415 V/50Hz output of the PMSG-SST but its High frequency transformer operates at 1KHZ. Then the microgrid distribute the microgrid load.

When excess power in microgrid, GRID-SST absorb power from the microgrid and converted 11KV, 50HZ supply. GRID-SST delivered power to central grid 3KW/0.25KVAR load at that condition Central grid main source will be off position. When the wind generation power is goes to zero. Central controller is decided to changeover the central grid source and its disconnect the PMSG-SST The wind turbine system and generator parameters are given in Table I.

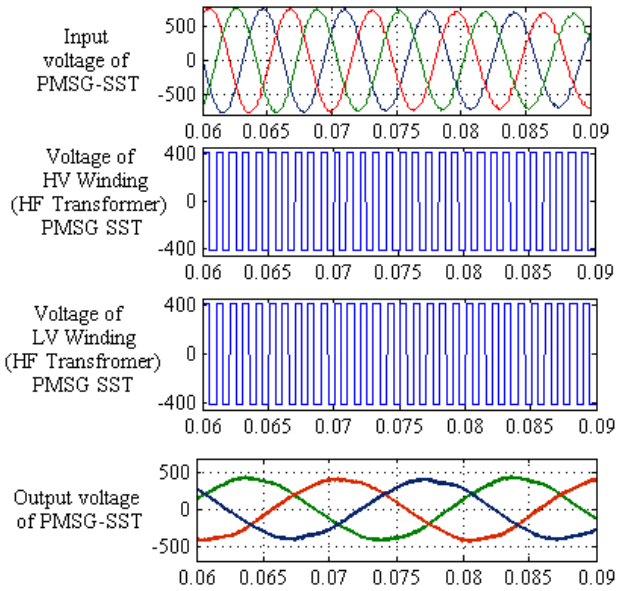

Fig.12. Simulation wave form of PMSG-SST High frequency transformer input Voltage, output voltage and PMSG-SST input Voltage, output voltage

B. PV generation mode

The PV system is modeling based on the equivalent circuit model which has already state in theory section. When the PV generation unit is operating with MPPT control, the maximum power is 10KW and the corresponding MPPT voltage is about 415V. PV (dc) voltage is converted into 3ph ac 415 voltage through Solar-SST but its High frequency transformer operates at 1KHZ. Solar-SST is connected into AC microgrid. Then microgrid distribute the microgrid load. When excess power in microgrid, GRID-SST absorb power from the microgrid and converted 11KV, 50HZ supply. GRID-SST delivered power to central grid 3KW/0.25KVAR load at that condition Central grid main source will be off position.. When the PV generation power is goes to zero. Central controller is decided to changeover the Central grid source and its disconnect to the Solar-SST. The PV system parameters are given in Table II.

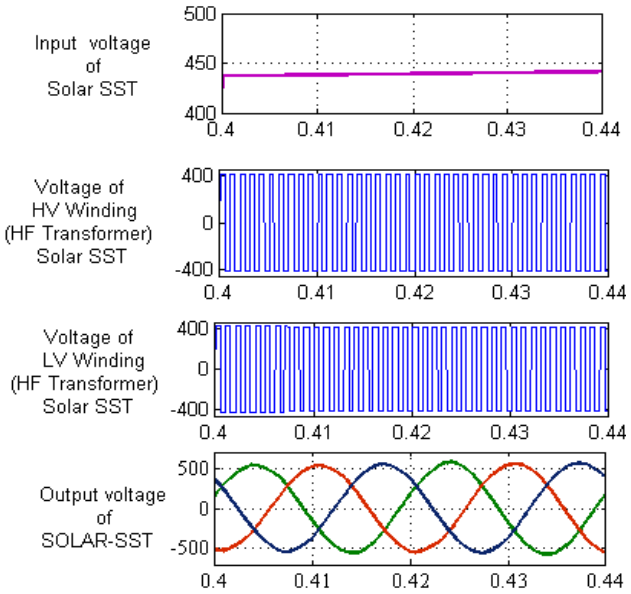

Fig.13. Simulation wave form of Solar-SST High frequency transformer input Voltage, output voltage and Solar-SST input Voltage, output voltage

C. Grid connection mode

When the wind generation and PV generation power is goes to zero. Central controller is decided to changeover the grid source and its disconnect the Solar-SST, PMSG-SST. Grid source is supplied to power the central grid 3KW load and AC microgrid power gets from Central grid through GRID-SST. Then microgrid distributes the microgrid load.

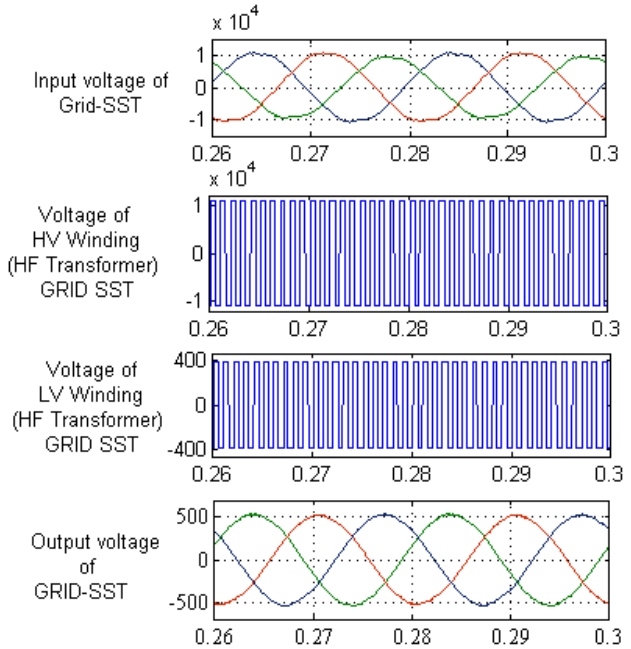

Fig.14. Simulation wave form of GRID-SST High frequency transformer input Voltage, output voltage and GRID-SST input Voltage, output voltage

D. Results

Wind Generation mode, PMSG system operate at 0 to 0.25 sec. 10KVA,415V PMSG supplies power to the microgrid through PMSG-SST.PMSG-SST is maintaining the 415 V/50Hz output of the PMSG-SST. In fault condition at 0.10 sec to 0.15 sec, at that condition microgrid load is affected but PMSG will not. Because PMSG-SST is electrically isolated. GRID-SST is maintaining the 11KV/50Hz output of the GRID-SST.

PV Generation mode PV system operate at 0.4 to 0.6 sec. 10KW,415V PV system supplies power to the microgrid through Solar-SST. Solar-SST is maintaining the 415 V/50Hz output of the Solar-SST. In fault condition at 0.50 sec to 0.55 sec, at that condition microgrid load is affected but PV will not. Because Solar-SST is electrically isolated. GRID-SST is maintaining the 11KV/50Hz output of the GRID-SST.

Grid connection mode, Central grid source operate at 0.25 to 0.4 sec. and 0.6 to 0.8 sec. 10KVA, 11KV Central grid supplies power to the microgrid through GRID-SST. GRID-SST is maintaining the 415 V/50Hz output of the GRID-SST. In fault condition at .10 sec to 0.15 sec and 0.50 sec to 0.55 sec, at that condition central grid will not be affected, because GRID-SST is electrically isolated.

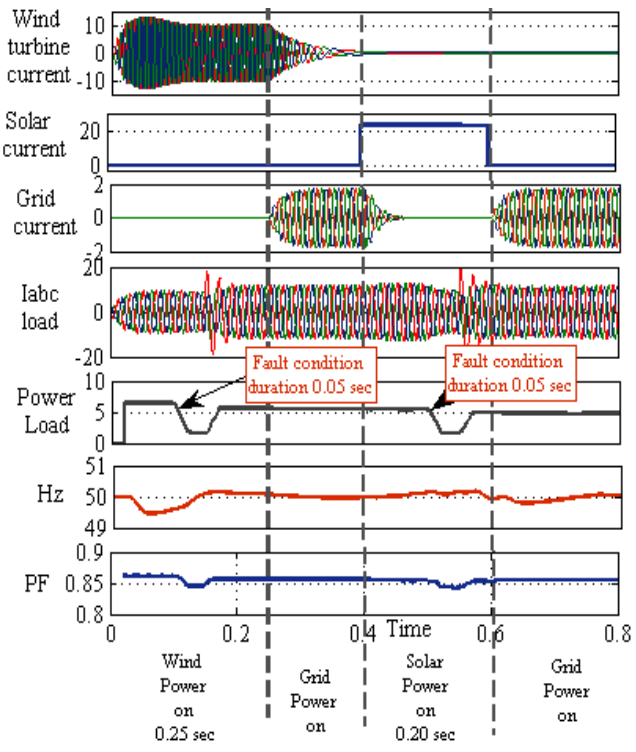

Fig.15. Simulation result of SST interfaced PMSG wind and PV based microgrid system connected with microgrid load.

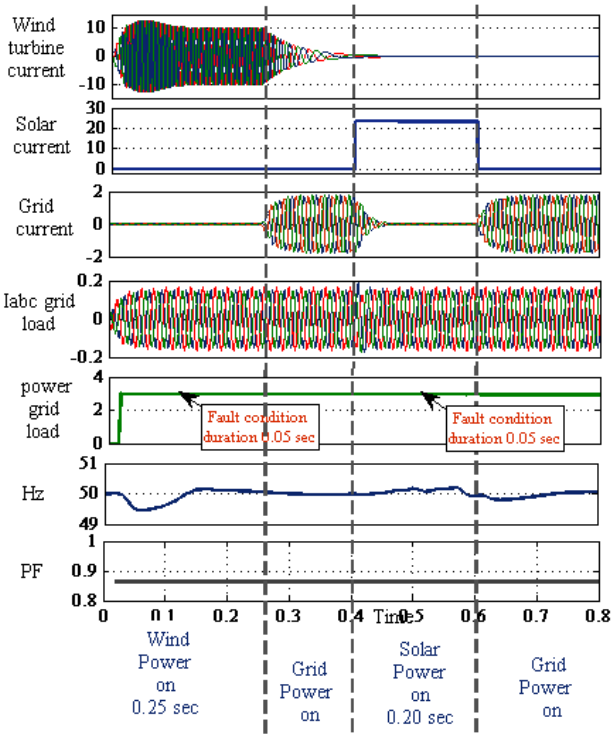

Fig.16. Simulation result of SST interfaced PMSG wind and PV based microgrid system connected with central grid load.

The SST protection scheme for the output short circuit is, the SST will stay online but limit the load current to 2 times of the rated current. Then some of the electronic equipment loads are not affected and still able to operate under a lower voltage. After the circuit breaker (or fuse) trip the fault, the SST will again output rated voltage. One of the most important features of the SST is the voltage sag or swell ride through capability. SST will support to maintain the 50Hz frequency and desired power factor in AC microgrid system.

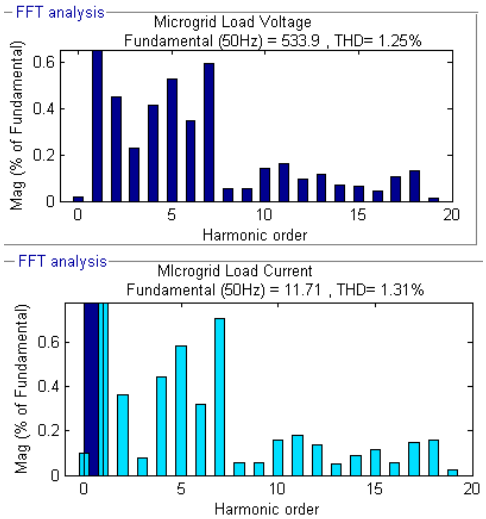

Fig.17. FFT Analysis of microgrid load.

Total harmonics disortion(THD) voltage in 1.25%
Total harmonics disortion(THD) current in 1.31 %

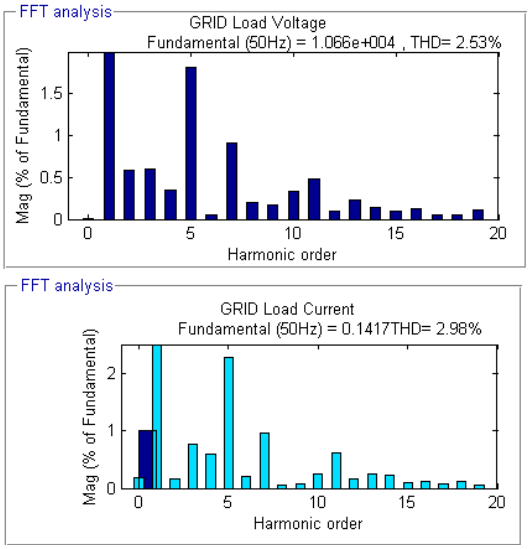

Fig. 18. FFT Analysis of central grid load.

Total harmonics disortion(THD) voltage in 2.53%
Total harmonics disortion(THD) current in 2.98 %

.

TABLE I

WIND TURBINE SYSTEM AND GENERATOR PARAMETERS

Wind turbine rated power	10KW	Generator rated power (Base)	10KW
Base wind speed	12 m/s	Generator rated speed	152.8 rad/s
Shaft stiffness constant (p.u.)	0.3	Generator rated voltage	415V
Shaft damping coefficient (p.u.)	1	Torque electrical	32.75 Nm
blade pitch angle	1	Torque Mechanical	33.95 Nm
Air density	1.225 kg/m^3		

TABLE II

PHOTOVOLTAIC SYSTEM PARAMETERS

Open-circuit voltage(Voc)	513.6 V
Short-circuit current(Isc)	23.84 A
Voltage at maximum power(Vmp)	437.9 V
current at maximum power(Imp)	22.32 A
Maximum Power(Pmp)	10439.53W

V ACKNOWLEDGMENT

The author thanks the institution of the Anna University, Regional campus, Madurai,Tamilnadu. for their continued support and encouragement throughout the course of the project.

REFERENCES

[1] Xunwei Yu, Xu She, ,Xijun Ni, and Alex. Q. Huang,“ System Integration and Hierarchical Power Management Strategy for a Solid-State Transformer Interfaced Microgrid System”, *IEEE Trans Power Electronics, Vol. 29, No. 8*, August 2014.

[2] W. van der Merwe and T. Mouton, “Solid-state transformer topology selection,” in *2009 IEEE International Conference on Industrial Technology*, 2009, pp. 1–6.

[3] S. Falcones and R. Ayyanar. (2010), “Topology comparison for Solid State Transformer implementation,” in IEEE PES General Meeting, pp. 1–8.

[4] M. Sztykiel, “Overview of Power Converter Designs Feasible for High Voltage Transformer-Less Wind Turbine,” in *IEEE* International Symposium on Industrial Electronics, 2011, pp. 1420-1425.

[5] Ch.Kalpana, Ch.SaiBabu, J.SuryaKumari. (2013), ‘Design and Implementation of different MPPT Algorithms for PV System’, International Journal of Science, Engineering and Technology Research, Vol.2, Issue 10.

[6] Xu She, Alex Q. Huang, Fei Wang, and Rolando Burgos, “Wind Energy System With Integrated Functions of Active Power Transfer, Reactive Power Compensation, and Voltage Conversion”, IEEE transactions on industrial electronics, vol. 60, no. 10, October 2013.

[7] X. She, X. Yu, F. Wang, et al, *Design and Demonstration of a 3.6-kV-120-V/10-kVA solid-state transformer for smart grid application*, IEEE Transactions on Power Electronics, Vol. 29, No. 8, pp. 3982-3996, Aug. 2014.

[8] F. Blaabjerg, K. Ma, “Future on Power Electronics for Wind Turbine Systems,” *IEEE Journal of Emerging and Selected Topics in Power Electronics*, vol. 1, no. 3, pp. 139-152, Sep. 2013.

[9] Tiefu Zhao, JieZeng, Subhashish Bhattacharya, Mesut E. Baran, Alex Q. Huang. (2009), ‘An Average Model of Solid State Transformer for Dynamic System Simulation’ 978-1-4244-4241-6/09/ IEEE.

[10] Xu She, Alex Q. Huang and Rolando Burgos, “Review of Solid-State Transformer Technologies and Their Application in Power Distribution Systems”, IEEE Journal of Emerging And Selected Topics In Power Electronics, Vol. 1, No. 3, pp.-186-198, September, 2013.

[11] Yazhou Lei, Alan Mullane, Gordon Lightbody, and Robert Yacamini, “Modeling of the Wind Turbine With a Doubly Fed Induction Generator for Grid Integration Studies” IEEE Transactions on Energy Conversion, Vol. 21, No. 1, March 2006.

[12] Rui Gao, Iqbal Husain, Fei Wang, and Alex Q. Huang, “Solid-State Transformer Interfaced PMSG Wind Energy Conversion System”, FREEDM systems center, Applied Power Electronics Conference and Exposition(APEC),2015 IEEE, 1310 – 1317, 15-19 March 2015.

[13] Qingshan wang, Xianning, Deliang Liang, “Characteristics research of wind power generator interfaced to grid via solid state transformer with energy storage device”, Ecological Vehicles and Renewable Energies(EVER), 2015 Tenth International Conference , 1 – 6, March 31 2015-April 2 2015.

[14] SubhadeepPaladhi , S. Ashok, “Solid state transformer application in wind based DG system” , Signal Processing, Informatics, Communication and Energy Systems (SPICES), 2015 IEEE International Conference , 1 – 5, 19-21 Feb. 2015.

[15] Muhammad H. Rashid ,Power electronics handbook : devices, circuits, and applications handbook ,Third edition 2011.

Sathishkumar R, Working as Lecturer in Anna University, Regional Campus at Madurai. Completed his Post graduate in power system engineering at Government college of Technology, Coimbatore, Completed his bachelor of engineering in Electrical and electronics engineering at Sethu Institute of Technology, Kariapatti. His area of interests are power systems, Smart grid, Renewable Energy sources.

Chandrasekaran V received his B.E in electrical and electronics Engineering from Thiagarajar college of engineering, Madurai, India in 2012. He is currently pursuing his PG in the *Department of Power systems engineering*, AnnaUniversity, Regional Office, Madurai, Tamilnadu,India. his area of interest includes Power system and Microgrid.

V Malathi received her Bachelor of Engineering in Electrical and Electronics from College of Engineering Guindy, Anna University, Chennai, and Master of Engineering in Power Systems from Thiagarajar College of Engineering, Madurai, Tamilnadu, India. She is a member of Institution of Engineers (India) and Life Member of the Indian Society for Technical Education. She is working as Professor in Department of Electrical and Electronics Engineering, Anna University, Regional Campus, Madurai, Tamilnadu, India. Her area of research is intelligent techniques applications to power system protection.